Interference in IM/DD Optical Wireless Communication Networks

Michael Rahaim and Thomas D. C. Little

***Abstract*—The emerging field of optical wireless communications (OWC) offers exceptional promise as a technology for next-generation wireless networks. High data rate capabilities and ultra-dense access point deployment will allow OWC to supplement traditional RF technologies and remove congestion from the crowded RF spectrum. When implementing OWC via intensity modulation with direct detection (IM/DD), peak optical power emission constrains the instantaneous optical power. Average optical power is also constrained by eye safety regulations and illumination requirements of infrared and visible light communication (VLC) systems, respectively. These constraints differ from the conventional electrical power constraint of RF and wireline systems. Accordingly, performance metrics such as signal-to-noise ratio (SNR) and signal-to-interference-plus-noise ratio (SINR) have been redefined in relation to the optical channel constraints in order to provide fair comparison across OWC implementations. In densely deployed networks, interference has a significant effect on system performance. Two key properties simplify the analysis of RF networks: 1) the relationship between electrical power and interference variance is modulation agnostic and 2) many interferers are typically assumed. The former allows SINR to be defined in terms of the channel constraint and the latter allows the aggregate disturbance from interference-plus-noise to be modeled as an additive Gaussian random component. In OWC networks, the optical power constraints relate to interference variance in a modulation specific manner, and the highly directional optical channel creates instances where a small set of interferers dominate the aggregate disturbance. In this work, we first derive bounds on the variance of OWC interference under the constraints of an OWC channel. We then evaluate the accuracy of assuming that interference follows a Gaussian distribution. Finally, we show results of a study in a testbed environment with 15 VLC-enabled LED luminaires in order to empirically evaluate OWC interference characteristics.**

***Index Terms*—Interference; Optical channel; Optical wireless communications; Signal-to-interference-plus-noise ratio (SINR); Software defined visible light communication (SDVLC).**

I. Introduction

The wireless communications industry is preparing for a substantial growth in wireless data demand from next-generation (5G) wireless devices and services. In particular, the increasing density and demand within indoor environments will continue to push the limits of our current RF-based wireless solutions. At the same time, optical wireless communications (OWC) technology is approaching a state of broad-scale commercial viability. There has been interest in OWC for indoor wireless data distribution since the 1970s [1–3]; however, improvements in LED technology and the growing adoption of LED-based indoor lighting has drawn attention to visible light communication (VLC) as an emerging OWC technology for 5G [4–6]. The capabilities of OWC make it a promising technology to supplement RF networks in the 5G ecosystem [7–9].

As the OWC field has developed, the primary focus of the community has been increasing link capacity in order to compete with RF technologies. These research activities have led to high-speed OWC implementations achieving Gb/s data rates [10,11]. In addition to competitive data rates, OWC also benefits from a highly directional emission profile that allows densely distributed OWC access points (APs) to achieve a high degree of spatial reuse. The signal directionality leads to a small per-cell coverage area at the working surface. Combining this highly localized signal emission with dense AP deployment provides excellent area-spectral efficiency ($b/s/m^2$). Densely distributed user entities (UEs) can then simultaneously utilize the optical channel's resources, which increases the network's aggregate capacity.

Ideal deployment of ultra-dense OWC networks should optimize the spatial reuse factor among APs while meeting the coverage requirements throughout the environment. Whenever overlap is required, it is important to characterize the interference between cells in order to determine if resource allocation is necessary or if UEs can maintain reliable communication in the presence of disturbances from interfering signals. In RF networks, interference analysis is simplified with two common assumptions. First, the RF channel constraint is on electrical power, which is directly related to the signal variance. Given the constraint of a known interferer and its channel response, the variance of the interfering signal can be evaluated without knowledge of the interfering signal's modulation and coding scheme. Accordingly, the variance of the aggregate disturbance from noise and interference can be determined by summing the individual variances.[1] Second, RF interference is typically assumed to be normally distributed due to the summation of many interfering signals; therefore,

Manuscript received February 7, 2017; revised June 10, 2017; accepted June 14, 2017; published August 15, 2017 (Doc. ID 284469).

M. Rahaim (e-mail: mrahaim@bu.edu) and T. D. C. Little are with the Engineering Research Center for Lighting Enabled Systems and Applications (LESA) and the Electrical and Computer Engineering Department, Boston University, Boston, Massachusetts 02215, USA.

https://doi.org/10.1364/JOCN.9.000D51

[1]Variance of the aggregate disturbance is equal to the sum of individual variances when noise and interference sources are independent and additive.

the aggregate disturbance from additive white Gaussian noise (AWGN) and interference is also normally distributed. This allows the signal-to-noise ratio (SNR) and signal-to-interference-plus-noise ratio (SINR) to be used interchangeably in error rate analysis.

In our previous work, we have shown preliminary analysis indicating how these assumptions can lead to inaccurate evaluation in the case of OWC systems implementing intensity modulation with direct detection (IM/DD). Given the optical power constraints of an IM/DD OWC link, the relationship between the channel constraint and signal variance is modulation dependent [12]. We have also shown how the directionality of the OWC channel tends toward conditions where a single dominant interferer exists and the distribution of the interference follows that of the modulated signal [13].

In this paper, we analyze OWC interference scenarios, evaluate the assumption that interference is normally distributed, and present bounding conditions on the interference variance and SINR under the constraints of an OWC channel. Section II provides an overview of interference conditions in OWC networks. Sections III and IV describe the OWC channel model and analysis characteristics. Section V defines bounding conditions for variance and SINR in IM/DD OWC networks under the constraints of an OWC channel. Section VI analyzes the effect of inaccurately assuming normally distributed interference and evaluates cases when the assumption is not appropriate for OWC. Section VII offers results of interference characterization in a testbed environment with 15 VLC enabled luminaires, and Section VIII concludes the paper.

II. OWC Interference

Interference occurs when multiple OWC signals land on the active area of a single UE's receiver. If the interfering signals are not accounted for, they add perturbations to the signal from the associated AP. In combination with random noise, these disturbances degrade the quality of the connection and negatively affect link performance. Understanding the characteristics of the interference allows for probabilistic modeling of link performance and the impact of interference; however, inaccurate assumptions about the interference characteristics can lead to inaccurate performance evaluation. Inaccurate models also present issues when comparing OWC links to other technologies in heterogeneous networks (HetNets).

The work presented in this paper can be used in other scenarios (e.g., device-to-device or mesh OWC networks); however, we are primarily concerned with the characterization of inter-cell interference in multicell OWC networks. These multicell networks include traditional lattice deployments as well as multitier OWC networks (e.g., VLC desk lamps operating under the coverage of VLC luminaires that are located at ceiling height) [14]. There is an extensive body of work that explores the effect of low-frequency disturbances from external optical sources, including DC ambient light (e.g., sunlight) and non-VLC lighting (e.g., fluorescent lights) [3]. In our work, these disturbances are considered as additive noise. Earlier work has also explored inter-symbol interference (ISI) caused by multipath reflections and symbol spreading [15]. We focus on interference related to additive optical power disturbances from other OWC devices.

A. Coverage and Interference Trade-Offs

When deploying an OWC network, there are trade-offs between the resource reuse factor and the coverage of the network. At one extreme, broad emission sources limit the outage regions in the environment and can guarantee with high probability that at least one OWC AP provides a suitable irradiance at the location of the UE. In this case, simultaneous transmission from neighboring APs may be restrictive. When signals from multiple APs land on the UE's photosensor, the system must either accept the disturbance caused by interfering signals or divide available resources among the APs such that the UE can distinguish between the signal transmitted by the associated AP and signals from interfering APs. At the other extreme, narrow emission sources can be deployed with limited overlapping regions in order to maximize the reuse factor. With narrow emission sources, there is a higher likelihood that a UE is placed in an area where an acceptable signal does not exist. These coverage gaps also increase the difficulty in accommodating mobility, since UEs pass through outage regions as they move from AP to AP. In addition, narrow emission sources are seldom considered when deploying dual-use VLC networks for lighting and data communications, since overlap is needed to meet the primary requirements of the lighting mission.

The receiver field of view (FOV) also affects the number of interfering APs seen by a UE, as depicted in Fig. 1. Given the directionality of the optical medium, the receiver's orientation has a high impact on the number of interfering APs within its FOV. Narrow FOV receivers have a higher probability of being placed or oriented in a way where no APs are within their FOV, whereas wide FOV receivers have a higher probability of having multiple APs within their FOV. Given the OWC channel's susceptibility to blocking, the number of interfering signals is also affected by obstructions (e.g., a user standing in the path between the AP and UE).

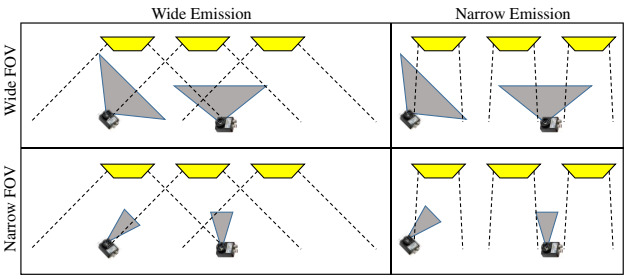

Fig. 1. Deployment classification (wide versus narrow emission; wide versus narrow FOV) for a single-input single-output (SISO) OWC network.

B. LOS and Multipath Interference

When multiple transmitting OWC APs fall within the FOV of the receiver, line-of-sight (LOS) interference occurs. This can include scenarios where resource allocation distinguishes between neighboring APs, but a receiver is rotated such that a far away AP with similar resources to the associated AP still falls within the FOV. LOS interference can also occur when resource allocation is used but the resources are not completely isolated. As an example, consider wavelength division multiplexing (WDM) or wavelength division multiple access systems where the transmitted optical power is not fully contained within the expected range of wavelengths. Here, interference occurs if signal from a neighboring color leaks into the spectral range of the expected color's optical filter.

Interference can also come from a non-associated AP that is outside the receiver's FOV. This occurs in scenarios where reflections off of objects in the environment cause the optical signal from an interfering AP to land on a UE's receiver through a multipath channel. In OWC, the multipath response typically has a much higher attenuation than the LOS response [16]. If the attenuation of the interfering signals drops the aggregate multipath interference below the noise floor, then the multipath response can be ignored. Similarly, LOS interference will typically dominate the aggregate multipath signal when one or more LOS interferers are present. Accordingly, the presence of a LOS interferer will tend to make the multipath interference negligible.

The received signal in a multipath environment will also undergo spreading in the time domain, which is the cause of ISI. This spreading will change the distribution of the interference and affect the relationship between the average received optical power and the variance of the aggregate optical signal from interfering APs. Additionally, the combination of multipath signals from many interferers allows the multipath interference to be viewed as an additive Gaussian disturbance. For these reasons, the work presented in this paper focuses on OWC interference characteristics in the dominant LOS interference scenarios that contradict the common interference assumptions in RF communications.

III. OWC Channel Model

The OWC signal chain is depicted in Fig. 2. We first discuss the signal chain for a single link in the absence of noise. A binary data stream, x_b, is first passed through an encoder to generate a discrete signal, $x[s]$. This is then sampled with a digital-to-analog converter (DAC) to generate the electrical signal, $x_{e_1}(t)$. This signal may then be carrier modulated and pre-processed to generate a positive valued electrical drive signal, $x_{e_2}(t)$, that is assumed to operate in the linear range of the optical conversion device. This signal is used to drive an optical source and generate the optical output consisting of the transmitted optical signal, $x^{(j)}(t)$, and any additional DC optical offset,[2] $P^{(j)}_{\mathrm{DC},tx}$. The superscript j indicates the jth AP when multiple APs are in the network. We use i in the general sense and j to indicate a specific AP under consideration.

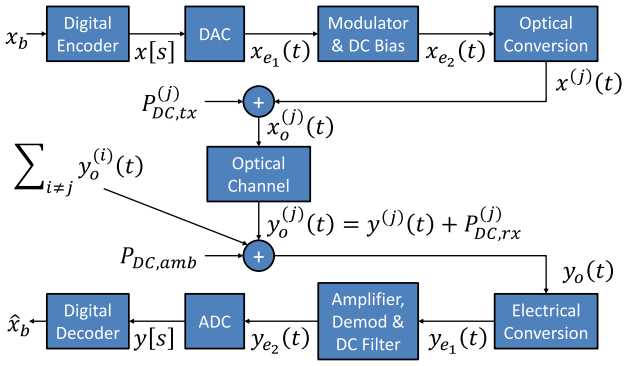

Fig. 2. Signal chain for an OWC link.

In the optical domain, $x^{(j)}(t)$ and $P^{(j)}_{\mathrm{DC},tx}$ pass through an optical channel. The received optical signal power is defined as $y^{(j)}(t)$, and the optical offset power from AP j is $P^{(j)}_{\mathrm{DC},rx}$. Additional optical power from other light sources also lands on the photosensor, combining with the received optical power from AP j to produce the total optical received power, $y_o(t)$. The additional optical power includes interfering signals from other APs in the environment, as well as any DC optical power from ambient and interfering sources. We also define $y^{(i)}_o(t)$ as the total optical power received from the ith AP.

At the receiver, $y_o(t)$ is converted back to the electrical domain, generating the DC biased electrical signal, $y_{e_1}(t)$, which is amplified, and filtered to produce the received electrical signal, $y_{e_2}(t)$. This signal is sampled at the ADC to generate a digital signal, $y[s]$. Finally, $y[s]$ is decoded in the digital domain in order to get the estimate of the original binary data stream, $\hat{x}_b$.

A. Optical Channel Response

In the analysis of an IM/DD OWC link, we are primarily concerned with the system beginning at the transmitted optical signal since various techniques can be used to implement the optical conversion. The optical channel impulse response, $h_o(t)$, specifies the channel and relates transmitted optical signal power to the optical signal power incident on the photosensor. It consists of a LOS component, $h_{o,\mathrm{LOS}}(t)$, and multipath component, $h_{o,m}(t)$:

$$y(t) = x(t) * h_o(t), \tag{1}$$

$$h_o(t) = h_{o,\mathrm{LOS}}(t) + h_{o,m}(t). \tag{2}$$

Given that the OWC frequency response is relatively flat near DC, the LOS component is defined by

$$h_{o,\mathrm{LOS}}(t) = VH_{o,\mathrm{LOS}}\delta(t-\tau), \tag{3}$$

where τ is the propagation delay and $H_{o,\mathrm{LOS}}$ is the DC LOS optical channel gain [3]. The visibility function, V, is set to

[2]The DC offset and $x^{(j)}(t)$ are separated such that $\min(x^{(j)}(t)) = 0$.

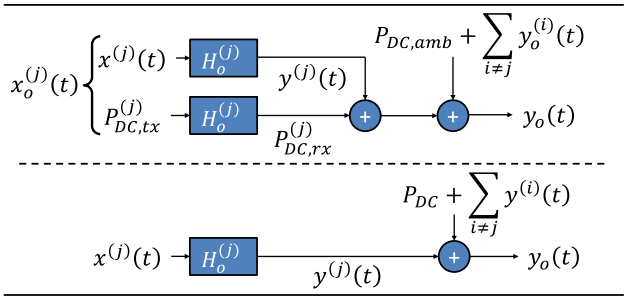

Fig. 3. Equivalent block diagrams for the optical signal chain.

1 if the LOS path exists and 0 if the path is occluded. Various models have been used to evaluate the multipath component; however, we ignore multipath for the reasons described in Subsection II.B and model the channel as

$$y(t) \approx x(t-\tau)VH_{o,\mathrm{LOS}} \equiv x(t)VH_{o,\mathrm{LOS}}, \tag{4}$$

where the equivalence assumes that the time shift is irrelevant.

As shown in Fig. 2, the total received optical power, $y_o(t)$, consists of the received optical signal, the summed interference from the set of interfering APs, and the sum of the various DC components, P_{DC}. We assume that, in the set of available APs, the AP that provides the largest received signal amplitude is associated with the receiver, and all other APs are considered interferers. Interfering signals follow a similar channel model, each with unique propagation delay and DC channel response.

At the receiver, an electrical current is generated proportional to $y_o(t)$. This proportionality factor is defined as the responsivity and is dependent on the spectral power distribution (SPD) of the light incident on the receiver as well as the receiver's wavelength-specific responsivity function. If $y(t)$ and P_{DC} do not have the same SPD, the responsivity to the signal, R [A/W], and to the DC optical power, R_{DC}, may differ. Total received current is then

$$y_{e_1}(t) = I_s(t) + \sum_i I_s^{(i)}(t) + R_{\mathrm{DC}}P_{\mathrm{DC}}, \tag{5}$$

where $I_s(t) = Ry(t)$ is the received electrical signal current from the associated AP and $I_s^{(i)}(t)$ is the signal current from the ith interferer.[3] The DC components of the associated and interfering signals are incorporated in the total DC optical power at the receiver. Combining these components simplifies the model and does not impact analysis since DC components of the original signals are not relevant when considering performance.[4] Equivalent block diagrams for the two models are shown in Fig. 3.

In order to relate analysis of the OWC channel to more conventional RF models, we have proposed a variant of the model in Ref. [18]. In the conventional view of IM/DD OWC,

[3]In the literature, the channel model often incorporates R in the channel response [17] such that $h(t) = Rh_o(t)$. Accordingly, this model must incorporate a unit conversion in the channel gain.

[4]DC optical power does not affect the signal in OWC, but does affect shot noise and may lead to saturation of the photosensor.

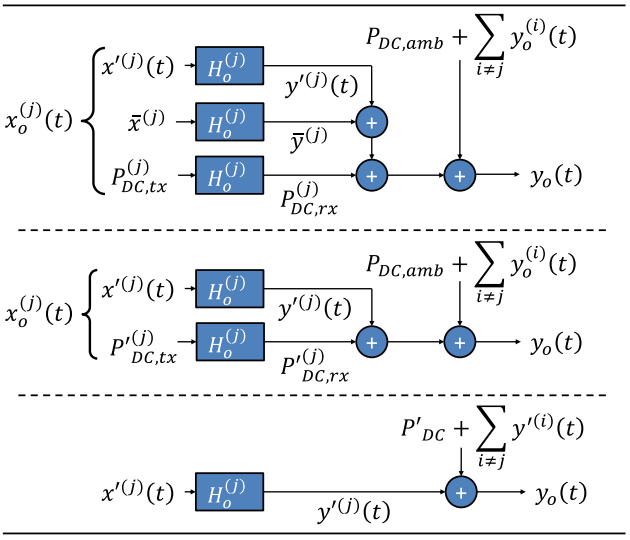

Fig. 4. Equivalent block diagrams for the variation of the optical signal chain, observing the unbiased signal, $x'(t)$.

the transmitted optical signal requires that $x(t)$ consists of a DC component to meet the positive value constraint; therefore, conventional symbol constellations must be translated to contain only positive values. The alternative model views the transmitted signal, $x'(t)$, as an optical power difference (i.e., the AC component) rather than an optical power output and is constrained by the peak-to-peak range rather than minimum and maximum values. With this definition, the received signal, $y'(t)$, is the optical power difference at the receiver. This allows $x'(t)$ to be defined as an unbiased signal such that $x'(t) = x(t) - \bar{x}$ and $y'(t) = y(t) - \bar{y}$.

Just as $P_{\mathrm{DC},tx}$ was defined as a component of P_{DC}, this model allows $\bar{x} = \mathrm{E}[x(t)]$ to be defined as a component of P'_{DC}, as shown in Fig. 4. This allows the signal, $x'(t)$, to be decoupled from the instantaneous optical power constraints under the assumption that a DC optical power, $P'_{\mathrm{DC},tx}$, is capable of shifting $x'(t)$ such that $\min(x'(t) + P'_{\mathrm{DC},tx}) \geq 0$. Figure 5 shows the components of $x_o(t)$ and $y_o(t)$ (excluding interference) for the biased and unbiased definitions of the optical signal.

Similar to the relationship between $I_s(t)$ and $y(t)$, we now define $I'_s(t) = Ry'(t)$ as the unbiased received electrical signal current. Note that the relationship between x and x' (as well as the corresponding received signal currents) implies that the variances are equivalent:

$$\sigma_x^2 = E[(x-\bar{x})^2] = E[(x')^2] = \sigma_{x'}^2, \tag{6}$$

$$\sigma_y^2 = E[(y-\bar{y})^2] = E[(y')^2] = \sigma_{y'}^2, \tag{7}$$

$$\sigma_{I_s}^2 = E[(I_s-\bar{I}_s)^2] = E[(I'_s)^2] = \sigma_{I'_s}^2. \tag{8}$$

This trait also holds when modeling the variance of the ith interferer in the same manner:

$$\sigma_{I_s^{(i)}}^2 = E[(I_s^{(i)}-\bar{I}_s^{(i)})^2] = E[(I_s'^{(i)})^2] = \sigma_{I_s'^{(i)}}^2. \tag{9}$$

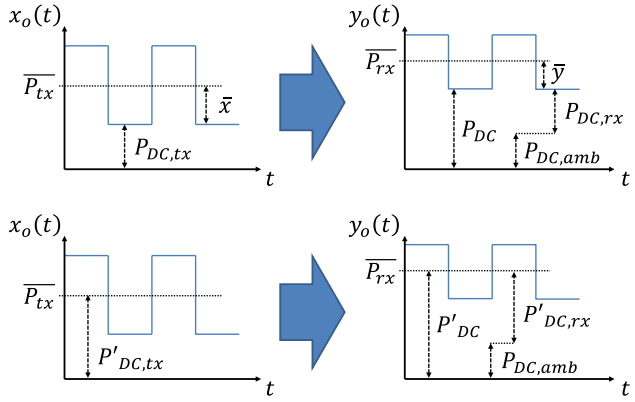

Fig. 5. Transmitted and received optical power with the conventional optical signal definitions, $x(t)$ and $y(t)$ (top) and with unbiased optical signal definitions, $x'(t)$ and $y'(t)$ (bottom). Interference is not shown.

In the signal chain from Fig. 2, the electrical signal to be sampled, $y_{e_2}(t)$, is an amplified version of $y_{e_1}(t)$ with filtering that is assumed to remove the additive DC component. This DC filtering removes the entire DC component, RP'_{DC}, which includes $\bar{I}_s$ and $\bar{I}_s^{(i)}$. This implies that the relevant observed signal is a superposition of the AC received signal components from the associated AP and interferers.

B. Noise Model

There are multiple noise components in an OWC link, with the dominant components being shot and/or thermal noise. Each is conventionally assumed to be independent and zero-mean AWGN. This allows the aggregate noise to be modeled as zero-mean AWGN with variance, σ_n^2, equal to the sum of the variances from the components. Other optical sources (e.g., fluorescent lighting) can also add random disturbance to the received signal. The primary difference between shot/thermal noise and noise from ambient light sources is that ambient sources tend to have a device-specific power spectral density [2] and cannot always be treated as white noise.

Since the various noise components occur throughout the signal chain, the equivalent noise is often defined at a specific location in the chain such that the various noise components can be combined as a single value. We consider the total noise as an additive electrical current at the output of the photosensor. This noise component has an electrical power, $P_{e,n}$, and variance, σ_n^2, that relates to the combined equivalent noise power and variance from all noise components if they were added at this point.

C. Interference Model

If the total interference is comparable or greater than the aggregate noise, it must be accounted for when evaluating signal disturbance. Given that interfering signals are independent, we define the variance of the combined interfering signal as

$$\sigma^2_{I_s^I} = \sum_{i \neq j} \sigma^2_{I_s^{(i)}} = \sum_{i \neq j} \sigma^2_{I_s'^{(i)}}, \tag{10}$$

where $I_s^{(j)}$ is assumed to be the signal current from the AP associated with the receiver.

In an OWC network, the amount of interference can vary drastically as interfering APs come in and out of the receiver's FOV and obstructions dynamically block the LOS path to different APs. Assuming that the associated AP has a LOS path, we can consider scenarios where a) all interference comes from the multipath components of interfering APs, b) one or more interferers have an unobstructed LOS path to the receiver and LOS interference dominates any interference from multipath components, or c) one or more LOS interferers exist and the aggregate interference from the multipath components of interfering APs is relevant. Given the characteristics of the LOS channel model, the variance of the interference from a LOS interferer is directly proportional to the variance of its transmitted optical signal; however, the variance of the interference from a multipath interferer will depend on the transmitted optical signal as well as environment characteristics. The discrepancies between OWC interference and RF interference are of particular interest for scenario b).

In a system with full duplex transmission, we assume that interference from the uplink channel of UEs in the environment contributes to the multipath interference at other UEs, and AP transmission contributes to the multipath interference at other APs. LOS interference is expected to occur at a UE when multiple APs are within its FOV and transmitting simultaneously, or at an AP when multiple UEs are within its FOV and transmitting simultaneously. In device-to-device networks, this assumption would not hold because devices may be simultaneously transmitting on a similar plane.

IV. OWC Channel Characteristics

Given the complexity of large wireless deployments, performance evaluation is often based on the characteristics of the system to make the analysis more tractable. In this way, channel quality metrics relate signal strength to signal disturbance (e.g., SNR or SINR) such that each is evaluated in terms of the channel constraints. The observed constraints should be defined such that fair comparison is provided across implementation parameters.

A. Channel Constraints

Conventionally, the signal in wireline or RF communications is subject to an electrical power constraint in the form $E[x_e^2(t)] \leq C_{P_e}$, where x_e is the electrical signal (i.e., voltage or current), and C_{P_e} is proportional to the maximum electrical power. When evaluating OWC networks, the primary constraints are different. In IM/DD optical systems, optical

power is constrained to positive values and the transmitter has a maximum instantaneous optical power [19]; therefore, transmitted optical power is constrained as $0 \le x_o(t) \le C_{tx,\max}$, where $C_{tx,\max}$ is the transmitter's maximum instantaneous optical power. In OWC, average optical power is also constrained due to eye safety regulations for IR or lighting requirements of dual-use VLC systems. Here, the additional constraint is in the form $E[x_o(t)] \le C_{tx,\text{av}}$, where $C_{tx,\text{av}}$ is the maximum average transmitted optical signal power [3,15].

In IR systems, regulations require average optical power to be below a specified maximum. In VLC systems, the lighting requirement specifies an average optical power that must be achieved, so average optical signal power may be combined with an additional DC bias to achieve the required average optical power. In this case, instantaneous optical signal power should be distinguished from the additional bias[2] in order to provide fair comparison.

When distinguishing between transmitted optical power and transmitted optical signal power, the constraints on $x_o(t)$ are directly related to constraints on $x(t)$. For a given minimum, $X_{\min} = \min(x_o(t))$, and maximum $X_{\max} = \max(x_o(t))$, we define the relationship $x(t) = x_o(t) - X_{\min}$ and the following signal constraints for the ith transmitter:

$$0 \le X_{\min}^{(i)} \le x_o^{(i)}(t) \le X_{\max}^{(i)} \le C_{tx,\max}^{(i)}, \tag{11}$$

$$0 \le x^{(i)}(t) \le X_{\max}^{(i)} - X_{\min}^{(i)} \le C_{tx,\max}^{(i)}, \tag{12}$$

$$\bar{x}^{(i)} = E[x^{(i)}(t)] \le E[x_o^{(i)}(t)] \le C_{tx,\text{av}}^{(i)}. \tag{13}$$

When the DC channel gain models the relationship between transmitted and received optical power, the constraints on a given transmitted signal can be directly related to the constraints on the received signal from the transmitting AP (defined in Table I):

$$0 \le Y_{\min}^{(i)} \le y_o^{(i)}(t) \le Y_{\max}^{(i)} \le C_{\max}^{(i)}, \tag{14}$$

$$0 \le y^{(i)}(t) \le Y_{\max}^{(i)} - Y_{\min}^{(i)} \le C_{\max}^{(i)}, \tag{15}$$

$$\bar{y}^{(i)} = E[y^{(i)}(t)] \le E[y_o^{(i)}(t)] \le C_{\text{av}}^{(i)}, \tag{16}$$

$$\bar{y}^{(i)} \le E[y_o^{(i)}(t)] \le E[y_o(t)]. \tag{17}$$

The additional upper bound in Eq. (17) relates to the superposition of the strictly positive received optical signal power, interfering signals, and the non-signal DC optical power (P_{DC}).

B. Channel Metrics

When evaluating system performance, the signal constraints are related to the variance of the random signal disturbance. The variance of the total disturbance from both noise and interference, σ_{tot}^2, is used for evaluating SINR:

$$\sigma_{\text{tot}}^2 = \sigma_{I_s^I}^2 + \sigma_n^2. \tag{18}$$

In observing Eq. (18), the approximation $\sigma_{\text{tot}}^2 \approx \sigma_n^2$ or $\sigma_{\text{tot}}^2 \approx \sigma_{I_s^I}^2$ is valid when $\sigma_n^2 \gg \sigma_{I_s^I}^2$ or $\sigma_{I_s^I}^2 \gg \sigma_n^2$, respectively. These scenarios allow either SNR or signal-to-interference ratio (SIR) to fully characterize the performance in noise-dominant or interference-dominant scenarios. Depending on the constraint, the signal quality of the associated AP can be defined in terms of average received electrical power, peak-to-peak signal range, or average received optical signal power:

$$\text{SINR}_{\bar{P}_e} = \frac{P_{e,\text{sig}}}{P_{e,I} + P_{e,n}} = \frac{\sigma_{I_s}^2}{\sigma_{\text{tot}}^2}, \tag{19}$$

$$\text{SINR}_{pp} = \frac{(R y_{pp}^{(j)})^2}{\sigma_{\text{tot}}^2} = \frac{I_{pp}^2}{\sigma_{\text{tot}}^2}, \tag{20}$$

$$\text{SINR}_{\bar{P}_o} = \frac{(R \bar{y}^{(j)})^2}{\sigma_{\text{tot}}^2} = \frac{\bar{I}_s^2}{\sigma_{\text{tot}}^2}. \tag{21}$$

In Eq. (19), $P_{e,\text{sig}}$, $P_{e,I}$, and $P_{e,n}$ are the AC electrical powers of the signal, interference, and noise, respectively. In Eq. (20), $y_{pp} = Y_{\max} - Y_{\min}$ is the peak-to-peak range of the received optical signal power, and I_{pp} is the peak-to-peak signal current. The definition in Eq. (20) is also often indicated in the optical domain such that it relates the optical power range to the standard deviation of the noise equivalent optical power. When observing average optical power constraints, the disturbance in Eq. (21) is occasionally modeled by the sum of σ_n^2 and the square of the average received optical power from interferers. In this case, the denominator no longer characterizes the variance of the disturbance in a general sense.

Extending the SNR relationships formed in Ref. [18], we can relate the SINR definitions from Eqs. (19)–(21) as follows:

$$\text{SINR}_{\bar{P}_o} = \frac{\bar{I}_s^2}{I_{pp}^2} \text{SINR}_{pp} = \frac{\bar{I}_s^2}{\sigma_{I_s}^2} \text{SINR}_{\bar{P}_e}. \tag{22}$$

TABLE I
OWC Transmit and Receive Parameters

Parameter	Tx Side	Rx Side (from AP i)
Total optical power	$x_o^{(i)}(t)$	$y_o^{(i)}(t) = H_o^i x_o^{(i)}(t)$
Avg. optical power	$P_{\text{DC},tx}^{(i)}$	$P_{\text{DC},rx}^{(i)} = H_o^i P_{\text{DC},tx}^{(i)}$
Max optical power	$C_{tx,\max}^{(i)}$	$C_{\max}^{(i)} = H_o^i C_{tx,\max}^{(i)}$
Max avg. optical power	$C_{tx,\text{av}}^{(i)}$	$C_{\text{av}}^{(i)} = H_o^i C_{tx,\text{av}}^{(i)}$
Optical signal power	$x^{(i)}(t)$	$y^{(i)}(t) = H_o^i x^{(i)}(t)$
Min optical signal power	$X_{\min}^{(i)}$	$Y_{\min}^{(i)} = H_o^i X_{\min}^{(i)}$
Max optical signal power	$X_{\max}^{(i)}$	$Y_{\max}^{(i)} = H_o^i X_{\max}^{(i)}$
Avg. optical signal power	$\bar{x}^{(i)}$	$\bar{y}^{(i)} = H_o^i \bar{x}^{(i)}$

C. Interference Metrics

When evaluating the effect of interference, we aim to determine when the system is operating under noise-dominant conditions, interference-dominant conditions, and conditions where the aggregate disturbance is highly dependent on both noise and interference. We also aim to relate the average optical power constraints of a single interferer to the noise power. Accordingly, we define the following metrics for interference-to-noise ratio (INR):

$$\mathrm{INR} = \frac{\sigma^2_{I_s'}}{\sigma^2_n}, \tag{23}$$

$$\mathrm{INR}^{(i)} = \frac{(R\bar{y}^{(i)})^2}{\sigma^2_n}. \tag{24}$$

In Ref. [12], we proposed the following definition for interferer-to-interference ratio (IIR) in order to evaluate the dominance of a single source of interference:

$$\mathrm{IIR} = \frac{\max_{i\neq j}(\bar{y}^{(i)})}{\sum_{i\neq j}(\bar{y}^{(i)})}, \tag{25}$$

where j represents the associated transmitter. IIR defines the percentage of the total interference related to the most dominant interferer and is of importance when evaluating the accuracy of assuming normally distributed interference.

V. Bounding SINR

As we have shown in Ref. [13], one of the key differences between the electrical power and average optical power constraints is that the relationship between variance and average optical power is dependent on the modulation. As an example, consider the received signal variance from a transmitter implementing pulse amplitude modulation (PAM) with M equally weighted and equidistant symbols in the range 0 to $2\bar{x}$:

$$\sigma^2_{x,\mathrm{MPAM}} = \frac{M+1}{3(M-1)}\bar{x}^2. \tag{26}$$

This shows that the relationship is dependent on the modulation order. Note that $\sigma^2_{x,\mathrm{MPAM}} = \bar{x}^2$ for an on-off keying (OOK) signal since $M = 2$.

The idea that σ^2_x can be bounded by $\bar{x}^2$ is disproven by considering variable pulse position modulation (VPPM). Given a VPPM signal with duty cycle α,

$$\sigma^2_{x,\mathrm{VPPM}} = \frac{1-\alpha}{\alpha}\bar{x}^2, \tag{27}$$

where a specified $\bar{x}$ can be achieved with any α in the range $0 \le \alpha \le 1$ when a peak value constraint is not known. With this relationship, $\sigma^2_{x,\mathrm{VPPM}}/\bar{x}^2$ can range from 0 to ∞. Therefore, the variance of an interfering signal cannot be bounded with knowledge of $\bar{x}^2$ alone.

A. Upper Bounds: Variance

Although the variance cannot be bounded with only knowledge of $\bar{x}$, Popoviciu's inequality bounds the variance of a signal constrained by a max and min value [20]. This bound can be tightened with additional knowledge of the mean [13]. We assume that the average optical power constraint must be met with equivalence such that $P'^{(i)}_{\mathrm{DC},tx} = C^{(i)}_{tx,\mathrm{av}}$.

(1) Define a signal, $z(t) = y^{(i)}_o(t) - \frac{1}{2}C^{(i)}_{\max}$ such that its magnitude is bounded by $\frac{1}{2}C^{(i)}_{\max}$ due to the constraints of Eq. (14) and, accordingly, $z(t)^2 \le \frac{1}{4}(C^{(i)}_{\max})^2$. Signals $y^{(i)}_o$, y, and z have equivalent variance bounded by

$$\begin{aligned}\sigma^2 &= E[z^2] - E[z]^2 \\ &\le \frac{(C^{(i)}_{\max})^2}{4} - \left(C^{(i)}_{\mathrm{av}} - \frac{C^{(i)}_{\max}}{2}\right)^2 \\ &= C^{(i)}_{\mathrm{av}}C^{(i)}_{\max} - (C^{(i)}_{\mathrm{av}})^2.\end{aligned} \tag{28}$$

(2) For an average optical power defined as a percentage of the maximum value constraint, $P'^{(i)}_{\mathrm{DC},rx} = \alpha C^{(i)}_{\max}$, we can rewrite the inequality from Eq. (28) as

$$\sigma^2 \le \alpha(1-\alpha)(C^{(i)}_{\max})^2. \tag{29}$$

(3) By repeating Step 1 with $z(t) = y^{(i)}(t) - \frac{1}{2}C^{(i)}_{\max}$ and observing the constraints of Eq. (15), the following bound is found in terms of $\bar{y}^{(i)}$ and is equivalent to Eq. (28) when no additional bias is added to the signal (i.e., $X^{(i)}_{\min} = 0$):

$$\sigma^2 \le \bar{y}^{(i)}C^{(i)}_{\max} - (\bar{y}^{(i)})^2. \tag{30}$$

(4) When repeating Step 1 with $z(t) = y^{(i)}(t) - \frac{1}{2}(Y^{(i)}_{\max} - Y^{(i)}_{\min})$ and observing the tighter constraints of Eq. (15),

$$\sigma^2 \le \bar{y}^{(i)}(Y^{(i)}_{\max} - Y^{(i)}_{\min}) - (\bar{y}^{(i)})^2. \tag{31}$$

(5) The bounds above are specific cases of the Bhatia–Davis inequality [21]. When min, max, and average values are known, the bound is formally defined by

$$\begin{aligned}\sigma^2_o &\le (Y^{(i)}_{\max} - C^{(i)}_{\mathrm{av}})(C^{(i)}_{\mathrm{av}} - Y^{(i)}_{\min}) \\ &= (Y^{(i)}_{\max} - \alpha C^{(i)}_{\max})(\alpha C^{(i)}_{\max} - Y^{(i)}_{\min}).\end{aligned} \tag{32}$$

Equations (28)–(32) bound the variance of interfering OWC signals in various ways, depending on the known constraints. Given no knowledge of the signal, Eqs. (28) and (29) bound the variance based on constraints of the channel. Given signal constraints (i.e., $Y^{(i)}_{\min}$, $Y^{(i)}_{\max}$, and/or $\bar{y}^{(i)}$), tighter bounds can potentially be found by using Eqs. (30)–(32). If the signal modulation is specified, σ^2 can be evaluated directly. Note that each inequality becomes unbounded if the average value is the only constraint and the other parameters are allowed to go to infinity (with the exception that $\sigma^2 = 0$ when $\bar{y}^{(i)} = 0$,

$C_{\text{av}}^{(i)} = 0$, $\alpha = 0$, or $\alpha = 1$). Additionally, Eq. (31) shows that $\sigma^2 \leq (\bar{y}^{(i)})^2$ is, in fact, the bounding condition when the peak-to-peak optical signal power is assumed to be $2\bar{y}^{(i)}$.

Given that variance of the interference from a single source is upper bounded, an upper bound on $\sigma^2_{I_s^I}$ can also be defined. Assuming that interfering signals are independent, the variance of the aggregate optical interference is the summation of the variances of the individual interferers and can be bounded in relation to the inequalities in Eqs. (28)–(32). As an example, the following inequality is defined in relation to Eq. (28):

$$\begin{aligned}\sigma^2_{I_s^I} &\leq \sum_{i\neq j}(R^{(i)})^2(C_{\text{av}}^{(i)}C_{\max}^{(i)} - (C_{\text{av}}^{(i)})^2)\\ &= \sum_{i\neq j}(H^{(i)})^2(C_{tx,\text{av}}^{(i)}C_{tx,\max}^{(i)} - (C_{tx,\text{av}}^{(i)})^2),\end{aligned} \tag{33}$$

where the second equality shows the bound when constraints are defined at the transmit side, and $H^{(i)} = R^{(i)}H_o^{(i)}$ represents the channel gain and unit conversion from the optical power at AP i to electrical current at the receiver. For generality in the case that SPDs are not equal across APs, we show $R^{(i)}$ as the responsivity of the receiver to the ith APs optical signal. If $C_{\text{av}}^{(i)}$ is defined as a percentage of the maximum value constraint, the following is similarly defined in relation to Eq. (29):

$$\begin{aligned}\sigma^2_{I_s^I} &\leq \sum_{i\neq j}(R^{(i)})^2\alpha^{(i)}(1-\alpha^{(i)})(C_{\max}^{(i)})^2\\ &= \sum_{i\neq j}(H^{(i)})^2\alpha^{(i)}(1-\alpha^{(i)})(C_{tx,\max}^{(i)})^2.\end{aligned} \tag{34}$$

B. SINR Upper and Lower Bounds

If the noise power is known, variance of the total disturbance can also be bounded by observing the bounds from the previous section offset by σ_n^2. As an example, consider the disturbance bounds that stem from Eqs. (33) and (34):

$$\sigma^2_{\text{tot}} \leq \sigma_n^2 + \sum_{i\neq j}(H^{(i)})^2(C_{tx,\text{av}}^{(i)}C_{tx,\max}^{(i)} - (C_{tx,\text{av}}^{(i)})^2), \tag{35}$$

$$\sigma^2_{\text{tot}} \leq \sigma_n^2 + \sum_{i\neq j}(H^{(i)})^2\alpha^{(i)}(1-\alpha^{(i)})(C_{tx,\max}^{(i)})^2. \tag{36}$$

If the constraints are equivalent across APs, then these bounds can be simplified even further:

$$\sigma^2_{\text{tot}} \leq \sigma_n^2 + (C_{tx,\text{av}}C_{tx,\max} - (C_{tx,\text{av}})^2)\sum_{i\neq j}(H^{(i)})^2, \tag{37}$$

$$\sigma^2_{\text{tot}} \leq \sigma_n^2 + ((C_{tx,\max})^2)\sum_{i\neq j}(H^{(i)})^2\alpha^{(i)}(1-\alpha^{(i)}). \tag{38}$$

Upper bounds on the total disturbance allow us to provide lower bounds on the SINR based on any of the definitions in Eqs. (19)–(21), as long as the quality of the associated signal is known. In addition, the SINR is upper bounded by the SNR given that the SNR is equivalent to the SINR when $\sigma^2_{I_s^I} = 0$.

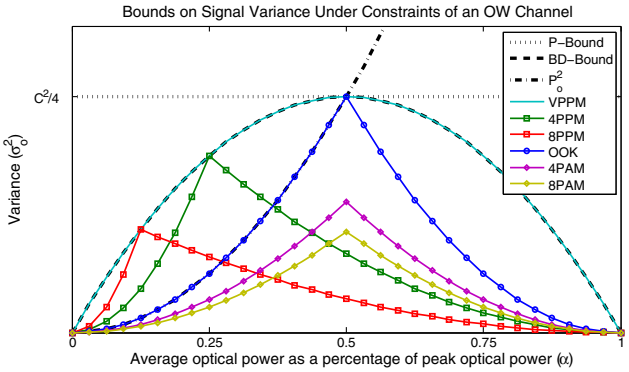

Fig. 6. Relationship between variance bounds (Popoviciu's and Bhatia–Davis) and calculated variance for various baseband modulation schemes. P_o^2 is the line indicating the squared average optical power.

SINR bounds do not provide a definitive performance evaluation; however, the bounds can provide valuable information about the network. In particular, evaluating the bounds on $\sigma^2_{I_s^I}$ will indicate conditions where the disturbance is guaranteed to be noise dominant. In such cases, interference can be ignored and performance evaluation with SNR is suitable. SINR bounds can also be used in the evaluation of HetNets. Given an OWC link with a lower bound on SINR, a minimum performance can be guaranteed. When comparing to an RF link with known performance, the OWC link is guaranteed to outperform the RF link in scenarios where the OWC link performance as evaluated with the bound is better than that of the RF link. However, the reverse cannot be definitively stated since the OWC link may still outperform the RF link in the scenarios where the RF link performance is better than the lower bound on the OWC link performance.

C. Simulation Results

To analyze the bounds described above, we present results from Ref. [13] that evaluate the true variance for a variety of common OWC modulation schemes and compare it to the bounding conditions. In Fig. 6, the bounding conditions are shown relevant to the variance of various pulsed modulation schemes. In Figs. 7 and 8, we compare the variance bounds to empirically determined variances for DC-biased optical orthogonal frequency-division multiplexing (OFDM) (DCO) and asymmetrically clipped optical OFDM (ACO) [22]. In both cases, we observe 64 subcarriers each implementing 16QAM and show post-clipping variance of the OFDM signals for various pre-clipping electrical powers.[5] The simulation is averaged over 1000 iterations of each combination of pre-clipping electrical power and

[5]Electrical power is defined as $\text{E}[y_o^2]$. The dBm values are relative to the maximum achievable electrical power given the peak constraint in Eq. (15).

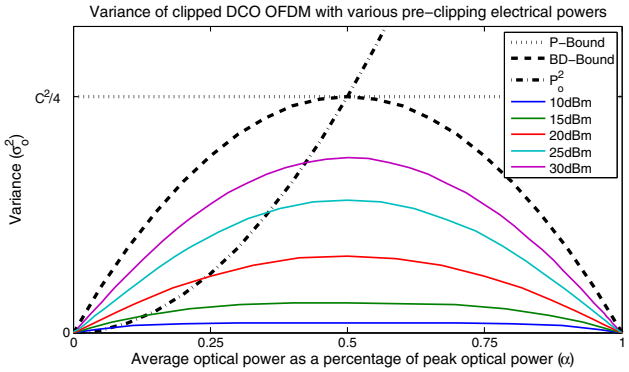

Fig. 7. Relationship between variance bounds and simulated variance for DCO signals with various pre-clipping electrical powers.

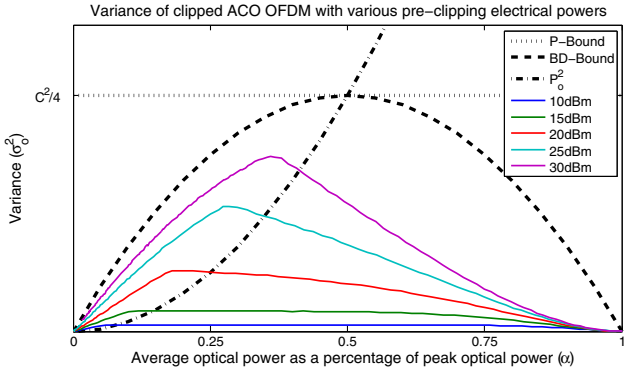

Fig. 8. Relationship between variance bounds and simulated variance for ACO signals with various pre-clipping electrical powers.

desired DC optical power scaled from well below the minimum clipping point to well above the maximum.

The results show that both the DCO and ACO techniques fall well below the Bhatia–Davis bound for practical pre-signal electrical powers. At 10 and 15 dBm, there is a range of α where the variance is constant. At these points, the signal fits within the boundaries of the OWC constraints and minimal clipping occurs. At 20 dBm, the DCO and ACO signals have minimal clipping at $\alpha = 0.5$ and $\alpha \approx 0.2$, respectively. However, shifting the desired average above or below these points can lead to large percentages of the signals being clipped. At 25 and 30 dBm, the signals see large clipping regardless of α.

VI. Gaussian Interference in OWC

Assuming that SINR can be evaluated with full knowledge of the system, it is often used for error rate analysis when the modulation and coding scheme of the associated AP is known. In the conventional use of SINR, the total disturbance is assumed to have a normal distribution due to the summation of many interferers and the central limit theorem. This allows SINR to be used in error rate calculations defined for SNR since the denominator in both cases

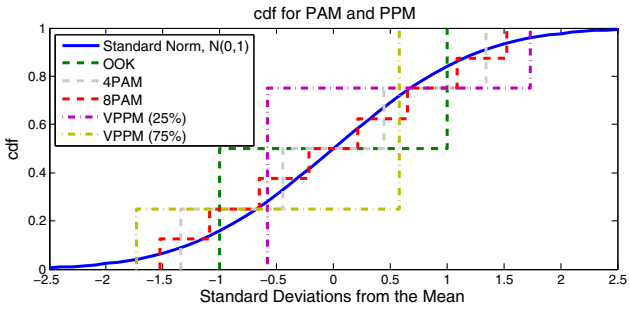

Fig. 9. Normalized distribution of baseband pulsed modulation schemes compared with a standard normal distribution.

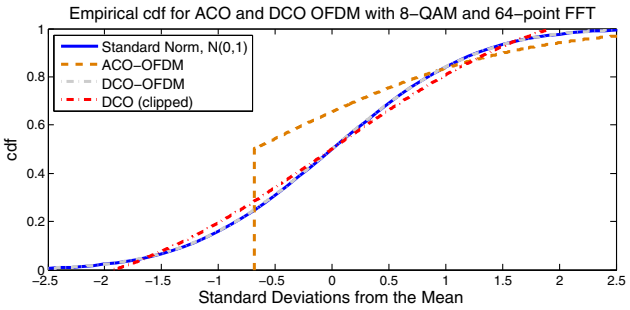

Fig. 10. Normalized distribution of time domain samples for DCO and ACO compared with a standard normal distribution.

is equivalent to the variance of a normally distributed signal disturbance. In the case of OWC, the directionality of the medium can lead to scenarios where a dominant interferer is the primary source of disturbance. In cases where the IIR is high and the INR indicates that interference is relevant to the disturbance, the distribution of the I_s^I follows close to the distribution of the dominant interferer.

In Figs. 9 and 10, we show results from Ref. [12] that analyze the disturbance of various pulsed modulation schemes and optical OFDM schemes. In each plot, the normalized distributions[6] of the described modulation schemes are compared with the standard normal distribution. Note that modulation schemes such as VPPM and ACO OFDM are not symmetrically distributed about the mean, implying that distributions have higher likelihood of shifting a signal in a certain direction, and the optimal decoding decision points are not the same as in the presence of strictly Gaussian disturbances. DCO OFDM signals are normally distributed; however, clipping in optical OFDM generates truncated normal distributions, and analysis is affected to various degrees depending on the clipping range.

A. Bit-Error-Rate Evaluation

To show how error rate analysis can be affected by inaccurately assuming normally distributed interference,

[6]The normalized distribution of the signal x is defined as $\frac{x-\mu_x}{\sigma_x}$, where μ_x and σ_x are the mean and standard deviation, respectively.

we evaluate the difference in the theoretical bit error rate (BER) for an OOK signal in the presence of a single dominant interferer that is also implementing OOK. True BER is derived for four equiprobable received values (0, $2\bar{y}^{(i)}$, $2\bar{y}^{(j)}$, and $2\bar{y}^{(i)} + 2\bar{y}^{(j)}$) through an AWGN channel. The average received interference power is $2\bar{y}^{(i)}$. Given a decision point at $\bar{y}^{(i)} + \bar{y}^{(j)}$, the true BER, BER_1, evaluates to

$$\text{BER}_1 = \frac{1}{2}Q\left(\sqrt{\text{SNR}} + \sqrt{\text{INR}^{(i)}}\right) + \frac{1}{2}Q\left(\sqrt{\text{SNR}} - \sqrt{\text{INR}^{(i)}}\right). \tag{39}$$

and the BER where conventional BER analysis of optical OOK is evaluated with SINR in the place of SNR is evaluated as

$$\text{BER}_2 = Q\left(\sqrt{\text{SINR}}\right). \tag{40}$$

B. Simulation Results

The differences between error rate calculations using BER_1 and BER_2 are depicted in Figs. 11 and 12. The figures from Ref. [12] show the relative error[7] (in dB) and the ratio (in dB) of the BER calculations, respectively. We use the relationship

$$\text{SINR} = \text{SNR}\left(\frac{\sigma_n^2}{\sigma_I^2 + \sigma_n^2}\right) = \text{SNR}\left(\frac{1}{\text{INR}^{(i)} + 1}\right), \tag{41}$$

where the second equality is valid for OOK due to the relationship $\sigma_{\text{OOK}}^2 = (R\bar{y})^2$ determined from Eq. (26). The range of INR shows the effect of interference between 1 order of magnitude above and below noise power. The SNR range relates to error rates between 10^{-2} and 10^{-8} in the absence of interference. Scenarios where $\text{INR}^{(i)} >$ SNR are not valid since the UE is assumed to be associated with the AP having maximum received signal.

In cases where $\sqrt{\text{SNR}} \pm \sqrt{\text{INR}^{(i)}} \approx \sqrt{\text{SINR}}$, we see that $\text{BER}_1 \approx \text{BER}_2$, and the assumption has minimal effect. This occurs when INR is low since noise dominates interference, $\text{SINR} \approx \text{SNR}$ and $\sqrt{\text{SNR}} \gg \sqrt{\text{INR}^{(i)}}$. When SNR is in the range of interest (i.e., 12 dB < SNR < 15 dB, where error rates from noise are between 10^{-5} and 10^{-8}) and interference either dominates or is on the same order of magnitude as noise power, relative error ranges from 0 dB (100%) to 20 dB (100×). As an example, BER_1 and BER_2 evaluate to approximately 3×10^{-5} and 3×10^{-3}, respectively, when $\text{INR}^{(i)} = 5$ dB and SNR = 15 dB. These values become further distorted as SNR increases beyond 15 dB.

VII. Experimental Evaluation

To validate the results from Refs. [12,13], we have developed a multicell VLC testbed, as shown in Fig. 13. The testbed is an extension of our previous work on software defined VLC (SDVLC) [23] with 15 Cree luminaires that have been modified to modulate an optical signal that is driven by the output of an Ettus Research universal software radio peripheral (USRP). Our analysis of interference involves eight of the APs surrounding TX 0, as shown in Fig. 14. In the evaluation, each transmitter is implementing 1 Mb/s OOK with a pseudo-random bit sequence. Measurements are taken at five locations below TX 0 with a Thorlabs avalanche photodiode (APD120A2) as the receiver. The locations, L_1 through L_5, are indicated in Fig. 15. We evaluate the distribution of the received interference when a) the receiver has both an optical lens (Thorlabs ACL25416U-B) and a 1 in. cone to narrow the FOV, b) the receiver has a cone but no lens, and c) the receiver has no cone or lens. In all three cases, an optical filter (Thorlabs FES500) is used to bandpass the signal in the blue spectrum.

Figures 16–18 show the resulting normalized distributions of the interference plus noise at an upward facing receiver for each of the three cases. The standard normal distribution is also shown for reference. In the case where the lens is used (Fig. 16), the interference plus noise follows

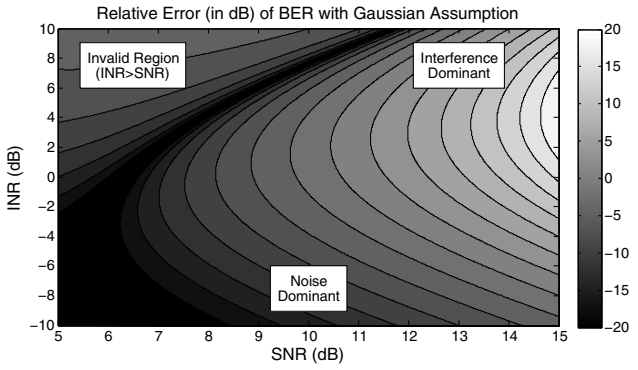

Fig. 11. Relative error (dB) in theoretical error rate of an OOK signal in the presence of interference from another OOK signal when using SINR and assuming Gaussian interference.

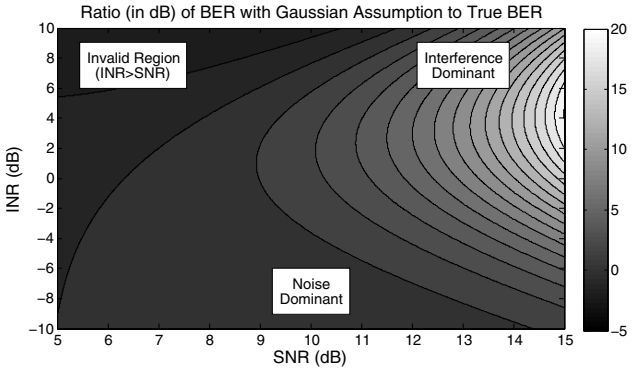

Fig. 12. Ratio (dB) of the theoretical error rate evaluated with SINR and assuming Gaussian interference to the true BER for an OOK signal in the presence of interference from another OOK signal.

[7]The relative error of BER_2 is defined as $\frac{|\text{BER}_2 - \text{BER}_1|}{\text{BER}_1}$.

Fig. 13. Dense deployment of VLC luminaires impacted by AP density and emission width as well as receiver FOV.

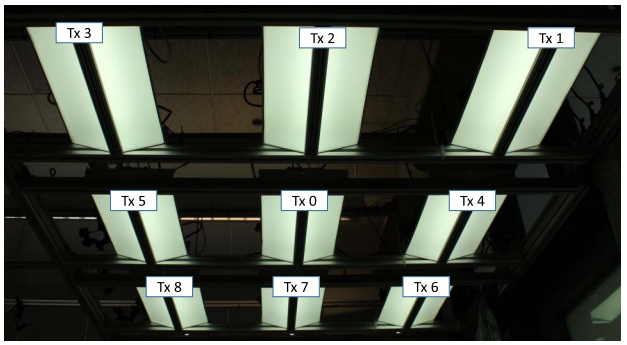

Fig. 14. Layout of luminaires for interference analysis.

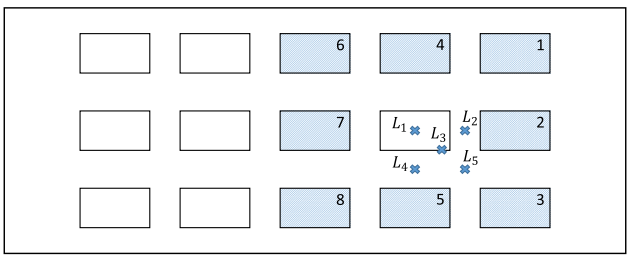

Fig. 15. Downward view of the SDVLC testbed indicating the five test points, L_1 through L_5, where the receiver is placed at table height.

closely to the normal distribution in all cases. This is due to the ability of the lens to focus light on the photosensor so that the interference is strictly multipath and is well below the noise floor. In this case, the system operates in a noise-dominant scenario and resources can be fully reused among APs; however, this also leads to many outage regions in the environment where the receiver is unable to receive signal from any APs.

In the case where no cone or lens is used (Fig. 17), the distribution of the interference also tends toward the normal distribution. This is due to the summation of the eight interfering signals. In this case, the interference can have a drastic impact on performance. The coverage in the environment is excellent as the receiver is able to view at least

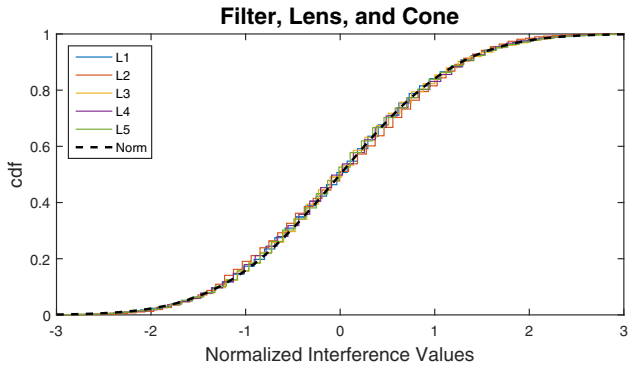

Fig. 16. Testbed results with a lens and cone for eight interfering signals at various locations in the environment.

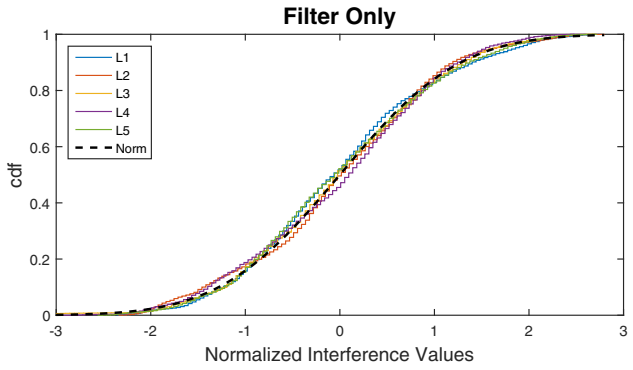

Fig. 17. Testbed results when no lens or cone is used for eight interfering signals at various locations in the environment.

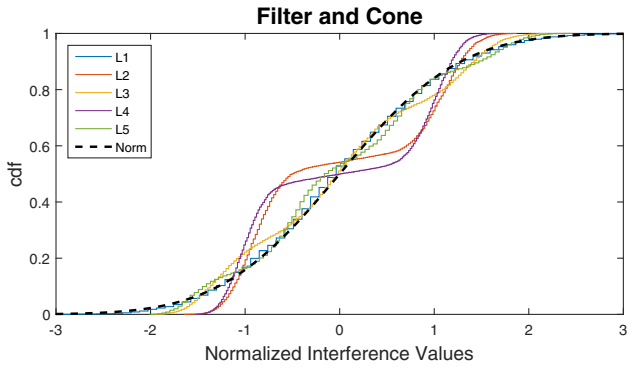

Fig. 18. Testbed results with a cone and no lens for eight interfering signals at various locations in the environment.

one AP throughout; however, the interference will require a high reuse factor to allow the receiver to distinguish between its intended signal and the interference from other devices.

Finally, when a cone is used to narrow the FOV (Fig. 18), the system is still able to achieve excellent coverage and the number of interferers is greatly reduced. In this case, the distribution of the total disturbance can vary greatly from the normal distribution since a small number

of interferers dominate the aggregate interference signal. At L_1, the resulting distribution is close to normal, since the cone causes the interfering APs to fall outside of the receiver's FOV. At L_3 and L_5, a somewhat stepped distribution is seen since APs 2, 3, and 5 all fall within the FOV. In this case, the distribution is trending toward normal due to summation of multiple interferers. At L_2 and L_4, a single interfering AP dominates the disturbance, and two discernible steps are seen in the distributions shown in Fig. 18. The interfering signals appear as the steps at approximately ± 1 standard distribution. Additional noise and any multipath interference leads to the distribution around those points. Note that the single dominant interferer scenario also occurs when occlusions block the LOS path to a subset of the interferers in situations where multiple LOS paths would otherwise be present.

VIII. Conclusion

The work presented in this paper shows the differences between interference in OWC networks and RF networks to indicate the potential impact of using conventional RF assumptions when modeling OWC network performance. In particular, we highlight multicell OWC networks with LOS interference as a specific area of interest for non-traditional interference models. System deployment parameters, including transmitter emission/layout and receiver FOV, will affect the occurrence of such scenarios; however, practical deployment should account for tradeoffs between the amount of LOS interference and coverage of the OWC network.

Given the OWC channel's susceptibility to blocking and the impact of device orientation, dynamic parameters such as the receiver's location/rotation and obstructions in the environment will also lead to such scenarios. In the case of dynamic parameters, system provisioning must account for non-traditional interference scenarios occurring with some probability. The exact probabilistic model for these dynamic parameters is expected to be highly dependent on the device type, use case, and environment, and is discussed as an area of further exploration in future work.

In this paper, we have provided a thorough description of the OWC signal chain in the presence of interference. We have also highlighted scenarios where common interference assumptions from the RF literature do not hold in a general case for OWC. Specifically, we have shown that the relationship between average optical power constraints and signal variance is not modulation agnostic and presented scenarios where the distribution of the OWC interference is not Gaussian. We have derived bounding conditions for the variance of interfering signals as well as the SINR under the constraints of an OWC channel, evaluated the effect of inaccurately assuming that interference in an OWC network is normally distributed, and presented results of interference distribution for a variety of receivers in a practical testbed environment. Accordingly, this work shows the importance of understanding the operating conditions when modeling the performance of OWC networks with dynamic UEs and evaluating the effect of interference.

Acknowledgment

This work was supported in part by the Engineering Research Centers Program of the National Science Foundation under NSF Cooperative Agreement No. EEC-0812056 and under Grant No. CNS-1617645. Portions of this work were presented at the ICC Workshops on Visible Light Communication and Networking (VLCN) and Optical Wireless Communications (OWC) in 2015 and 2016, respectively [12,13].

References

[1] F. R. Gfeller and U. Bapst, "Wireless in-house data communication via diffuse infrared radiation," *Proc. IEEE*, vol. 67, no. 11, pp. 1474–1486, Nov. 1979.

[2] A. C. Boucouvalas, "Indoor ambient light noise and its effect on wireless optical links," *IEE Proc. Optoelectron.*, vol. 143, no. 6, pp. 334–338, Dec. 1996.

[3] J. Kahn and J. Barry, "Wireless infrared communications," *Proc. IEEE*, vol. 85, no. 2, pp. 265–298, Feb. 1997.

[4] S. Wu, H. Wang, and C.-H. Youn, "Visible light communications for 5G wireless networking systems: From fixed to mobile communications," *IEEE Netw.*, vol. 28, no. 6, pp. 41–45, Nov. 2014.

[5] Z. Ghassemlooy, S. Arnon, M. Uysal, Z. Xu, and J. Cheng, "Emerging optical wireless communications—Advances and challenges," *IEEE J. Sel. Areas Commun.*, vol. 33, no. 9, pp. 1738–1749, Sept. 2015.

[6] M. B. Rahaim and T. D. C. Little, "Toward practical integration of dual-use VLC within 5G networks," *IEEE Wireless Commun.*, vol. 22, no. 4, pp. 97–103, Aug. 2015.

[7] M. B. Rahaim, A. Vegni, and T. D. C. Little, "A hybrid radio frequency and broadcast visible light communication system," in *IEEE GLOBECOM Workshops*, 2011, pp. 792–796.

[8] H. Chowdhury and M. Katz, "Cooperative data download on the move in indoor hybrid (radio-optical) WLAN-VLC hotspot coverage," *Trans. Emerging Telecommun. Technol.*, vol. 25, pp. 666–677, 2014.

[9] M. Ayyash, H. Elgala, A. Khreishah, V. Jungnickel, T. Little, S. Shao, M. B. Rahaim, D. Schulz, J. Hilt, and R. Freund, "Coexistence of WiFi and LiFi toward 5G: Concepts, opportunities, and challenges," *IEEE Commun. Mag.*, vol. 54, no. 2, pp. 64–71, Feb. 2016.

[10] D. Tsonev, H. Chun, S. Rajbhandari, J. J. McKendry, S. Videv, E. Gu, M. Haji, S. Watson, A. E. Kelly, G. Faulkner, M. D. Dawson, H. Haas, and D. O'Brien, "A 3-Gb/s single-LED OFDM-based wireless VLC link using a gallium nitride μLED," *IEEE Photon. Technol. Lett.*, vol. 26, no. 7, pp. 637–640, 2014.

[11] A. Gomez, K. Shi, C. Quintana, M. Sato, G. Faulkner, B. C. Thomsen, and D. O'Brien, "Beyond 100-Gb/s indoor wide field-of-view optical wireless communications," *IEEE Photon. Technol. Lett.*, vol. 27, no. 4, pp. 367–370, 2015.

[12] M. B. Rahaim and T. D. C. Little, "Optical interference analysis in visible light communication networks," in *IEEE ICC 2015—1st Workshop on Visible Light Communications and Networking (VLCN) (ICC'15—Workshops 24)*, London, UK, June 2015.

[13] M. B. Rahaim and T. D. C. Little, "Bounding SINR with the constraints of an optical wireless channel," in *IEEE Int. Conf. on Communications Workshops (ICC)*, May 2016, pp. 417–422.

[14] T. Borogovac, M. Rahaim, and J. Carruthers, "Spotlighting for visible light communications and illumination," in *IEEE GLOBECOM Workshops*, Dec. 2010, pp. 1077–1081.

[15] T. Komine and M. Nakagawa, "Fundamental analysis for visible-light communication system using LED lights," *IEEE Trans. Consum. Electron.*, vol. 50, no. 1, pp. 100–107, Feb. 2004.

[16] J. Carruthers and P. Kannan, "Iterative site-based modeling for wireless infrared channels," *IEEE Trans. Anntenas Propag.*, vol. 50, no. 5, pp. 759–765, 2002.

[17] H. Park and J. Barry, "Modulation analysis for wireless infrared communications," in *IEEE Int. Conf. on Communications, ICC '95, 'Gateway to Globalization'*, Vol. 2, 1995, pp. 1182–1186.

[18] M. B. Rahaim and T. D. C. Little, "Reconciling approaches to SNR analysis in optical wireless communications," in *IEEE Wireless Communications and Networking Conf. (WCNC)*, 2017.

[19] G. P. Agrawal, *Fiber-Optic Communication Systems*. Wiley, 1997.

[20] T. Popoviciu, "Sur les équations algébriques ayant toutes leurs racines réelles," *Mathematica*, vol. XI, pp. 129–145, 1936.

[21] R. Bhatia and C. Davis, "A better bound on the variance," *Amer. Math. Monthly*, vol. 107, pp. 353–357, 2000.

[22] J. Armstrong, "OFDM for optical communications," *J. Lightwave Technol.*, vol. 27, no. 3, pp. 189–204, Feb. 2009.

[23] M. B. Rahaim, A. Mirvakili, S. Ray, M. Hella, V. Koomson, and T. D. C. Little, "Software defined visible light communication," in *Wireless Innovations Forum Conf. on Wireless Communications Technologies and Software Defined Radio (SDR-WInnComm)*, 2014.

Michael Rahaim is a postdoctoral researcher in the Department of Electrical and Computer Engineering at Boston University and a member of the National Science Foundation Engineering Research Center for Lighting Enabled Systems and Applications (LESA). His current research focuses on next-generation wireless networks, software defined radio, and heterogeneous integration of wireless technologies including RF, OW, and VLC. Dr. Rahaim received his B.S. degree in electrical and computer engineering from Rensselaer Polytechnic Institute in 2007, and his M.S. and Ph.D. degrees in computer engineering from Boston University in 2011 and 2015, respectively. He is a Member of the IEEE and of the IEEE Communications Society.

Thomas D. C. Little is a professor in the Department of Electrical and Computer Engineering at Boston University. He is Associate Director of the National Science Foundation Engineering Research Center for Lighting Enabled Systems and Applications (LESA), a collaboration of Rensselaer Polytechnic Institute (RPI), the University of New Mexico, and Boston University. His current research focuses on pervasive computing using wireless technologies including applications in smart indoor environments, connected healthcare, and vehicular networking. Dr. Little received his B.S. degree in biomedical engineering from RPI in 1983, and his M.S. degree in electrical engineering and Ph.D. degree in computer engineering from Syracuse University in 1989 and 1991, respectively. He is a Senior Member of the IEEE, a member of the IEEE Computer and Communications Societies, and a member of the Association for Computing Machinery.